

Template-Directed Assembly of Receptor Signaling Complexes[†]

Anthony L. Shrout, David J. Montefusco, and Robert M. Weis*

Department of Chemistry, LGRT 701, 710 North Pleasant Street,
University of Massachusetts, Amherst, Massachusetts 01003-9336

Received July 18, 2003; Revised Manuscript Received September 26, 2003

ABSTRACT: Transmembrane receptors in the signaling pathways of bacterial chemotaxis systems influence cell motility by forming noncovalent complexes with the cytoplasmic signaling proteins to regulate their activity. The requirements for receptor-mediated activation of CheA, the principal kinase of the *Escherichia coli* chemotaxis signaling pathway, were investigated using self-assembled clusters of a receptor fragment (CF) derived from the cytoplasmic domain of the aspartate receptor, Tar. Histidine-tagged Tar CF was assembled on the surface of sonicated unilamellar vesicles via a lipid containing the nickel-nitrilotriacetic acid moiety as a headgroup. In the presence of the adaptor protein CheW, CheA bound to and was activated ~180-fold by vesicle-bound CF. The extent of CheA activation was found to be independent of the level of covalent modification on the CF. Instead, the stability of the complex increased significantly as the level of covalent modification increased. Surface-assembled CF was also found to serve as a substrate for receptor methylation in a reaction catalyzed by the receptor methyltransferase, CheR. Since neither CheA activation nor CF methylation was observed in comparable samples in the absence of vesicles, it is concluded that surface templating generates the organization among CF subunits required for biochemical activity.

The organization and asymmetry inherent in cell membranes creates an environment in which receptor proteins can effectively convey information between the inside and the outside of the cell (1). The reduction in the degrees of freedom experienced by transmembrane and peripheral membrane proteins provides a strong driving force for lateral organization, which can be essential for function (e.g., ligand-induced clustering (2)). These factors are in effect at the plasma membrane inner leaflet, where the assembly and regulation of signaling components often occur (3–5). In the chemotaxis signal transduction pathway of *Escherichia coli*, complexes of transmembrane receptors and cytoplasmic signaling proteins (6, 7) regulate protein phosphorylation through ligand–receptor interactions and receptor covalent modification (8–14). This transduction pathway is coupled to cell motility, which biases the swimming behavior of the cell in attractant and repellent gradients (15).

Several lines of evidence suggest that receptors for the bacterial chemotaxis pathway in *E. coli* are clustered in the cell membrane (16–18) and that close associations between receptors of different ligand specificity are important in signaling (19–23). This large class of bacterial receptors (24, 25) is also known as the methyl-accepting chemotaxis proteins (MCPs),¹ due to the enzyme-catalyzed receptor methylation and demethylation reactions that are essential for sensory adaptation (26). A structural model for the MCP dimer, which has been generated by Kim et al. from the crystal structures of the soluble domains (27), is shown in

Figure 1 and provides insights into the molecular basis for the requirement of receptor clusters in signaling. *E. coli* has four MCPs (Tar, Tsr, Tap, and Trg) and an aerotaxis receptor (Aer), which are distinguished primarily by ligand binding specificities that reside in the N-terminal domains. The dimeric organization of MCPs is evident in crystal structures of the aspartate receptor (Tar) ligand binding domain (28, 29) and the serine receptor (Tsr) cytoplasmic domain (27). The significantly greater homology among the C-terminal domains of these five receptors provides the basis for common interactions among a set of cytoplasmic signaling proteins (24), which generate the excitatory and adaptive responses to the chemotactic stimuli (reviewed in ref 30). In addition, the Tsr cytoplasmic domain is organized as a trimer-of-dimers in the crystal structure (27). The subunit interactions that lead to the trimer-of-dimer structure are apparently important for the intact receptor in the cell since mutations in conserved amino acid residues at the trimer-of-dimer contact site disrupt chemotaxis and receptor clustering (23). Thus, within the context of these heterogeneous receptor clusters, the overall CheA activity reflects the influences of the various independent inputs detected by the MCPs and Aer.

Biochemical investigations using membrane preparations of either Tar or Tsr with the purified signaling proteins have

[†] This work was supported through the NIH grant R01 GM53210 (R.M.W.).

* To whom correspondence should be addressed. Phone: (413) 545-0464. Fax: (413) 545-4490. E-mail: rmweis@chem.umass.edu.

¹ Abbreviations: MCP, methyl-accepting chemotaxis protein; Tar, aspartate receptor; Tsr, serine receptor; Tap, dipeptide receptor; Trg, ribose/galactose receptor; Aer, aerotaxis receptor; CF, cytoplasmic fragment; DOPC, 1,2-dioleoyl-*sn*-glycero-3-phosphocholine; DOGS-NTA, 1,2-dioleoyl-*sn*-glycero-3- $\{[N(5\text{-amino-1-carboxypentyl})\text{imino-diacetic acid}]\text{-succinyl}\}$ ammonium salt; DOGS-NTA-Ni²⁺, DOGS-NTA nickel salt; SUV, sonicated unilamellar vesicles; Ni-NTA, nickel-nitrilotriacetic acid; *tod*, trimer-of-dimer; SAM, *s*-adenosyl-L-methionine.

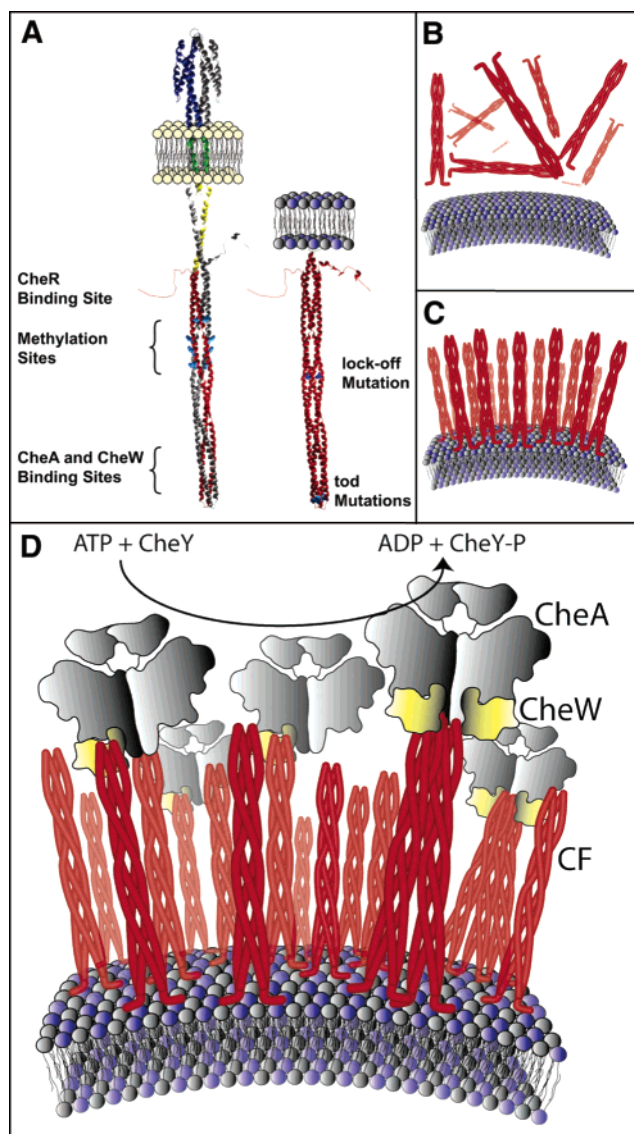


FIGURE 1: Receptor structure and surface-templated complex assembly. (A) The model of the chemotaxis receptor dimer at left is based primarily on the ligand binding and cytoplasmic domain crystal structures (27). One subunit is rendered in gray, and the other is color-coded to indicate functional regions: ligand binding domain (blue), transmembrane segments (green), linker region (yellow), and the cytoplasmic domain (red). The methylation sites (Q295, E302, Q309, and E491) are depicted with space-filling representations. The membrane-anchored CF dimer at right indicates positions of the S461L *lock-off* mutation and two *tod* mutations (E383A and E382P) in space-filling representation. (B–D) Cartoons depicting CF binding to the SUV surface. CFs are shown as dimers for simplicity.

clarified some of the properties of CheA activation and regulation (8–14). Notable observations include the substantial increase in CheA activity (>100-fold) that accompanies signaling complex formation, the stimulating influence of receptor methylation on CheA activity, and the inhibitory influence of ligand binding. However, membrane samples of the MCPs that are used in these biochemical experiments are frequently isolated from cells expressing the receptor at elevated levels, which can result in complex and heterogeneous samples (31). In addition, receptor reconstitution is labor-intensive, and the conditions that maintain a high level of activity while also preserving the vectoral and lateral organization required for function can be difficult to

find (32, 33). To circumvent the difficulties that typically plague the use of such samples, studies of CheA activation have used soluble receptor cytoplasmic fragments (CFs). In many instances the CFs are unable to activate CheA, but those that do activate CheA seem to do so via oligomerization, which occurs synergistically with CheW and CheA binding (34–37). While this approach has helped to elucidate the enzymatic properties of receptor signaling complexes, the formation of these complexes is limited to certain relative concentrations of CF, CheW, and CheA and is undesirably sensitive to variations in the tendency of different CFs to oligomerize. As a result, it has not been possible to study all the factors that are important for CheA activation.

We have developed a different approach for assembling signaling complexes that does not depend strongly on the propensity of the CF to self-associate, which has thus allowed us to study the formation of signaling complexes over a wide range of CheW concentrations. Sonicated unilamellar vesicles (SUVs) containing a nickel-chelating lipid (38) were used to template the assembly of histidine-tagged CF derived from *E. coli* Tar onto the outer leaflet of the membrane bilayer. The organization of CF produced by vesicle binding was found to resemble the environment of the cell membrane inner leaflet sufficiently well to promote the assembly of active (CF/CheW/CheA) signaling complexes and to restore enzyme-catalyzed methylation of the CF. The vesicle templating approach described here promises to be generally useful in situations where the signaling proteins require the organizing influence of the cell membrane to function.

MATERIALS AND METHODS

Protein Purification. The chemotaxis proteins CheA, CheR, CheW, CheY, and Tar CF were purified according to established protocols (11, 19, 39). Tar CF was expressed from the plasmid pHTCF (19), which generated a protein that contains residues 257–553 of *E. coli* Tar, a vector-encoded hexahistidine affinity tag at the N-terminus (MRGSHHHHHHGSPM₂₅₇), and the wild-type pattern of amidation (QEQE) at the methylation sites (Gln295, Glu302, Gln309, Glu491). pHTCF derivatives pSM100 and pSM101, which were used to produce CF in the deamidated (CF_{EEEE}) and fully amidated (CF_{QQQQ}) forms, respectively, were constructed with standard site-directed mutagenesis methods and verified by sequencing. Protein concentrations were determined with the Lowry assay according to the manufacturer's instructions (D_c Protein Assay, Bio-Rad Laboratories). Purified and concentrated proteins were flash frozen in liquid nitrogen and stored at –75 °C.

Assembly of Vesicle-Templated Signaling Complexes. SUVs were prepared from chloroform solutions of DOGS-NTA-Ni²⁺ and DOPC (Avanti Polar Lipids) in a 1:1 molar ratio, which were evaporated under a nitrogen stream until a dried lipid film was obtained. Assay buffer (pH 7.5, 75 mM Tris-HCl, 100 mM KCl, 5 mM MgCl₂, 2 mM TCEP, 5% DMSO) was added to produce a 2 mg/mL lipid concentration, the film was hydrated for 20 min at 25 °C, and then the sample was bath sonicated at 30 °C (Branson Model 2510) until the solution clarified (~70 min). Isothermal titration calorimetry was used to estimate that 60% of the DOGS-NTA-Ni²⁺ was in the outer leaflet of the SUV membrane and available for CF binding (data not shown).

This value was determined from the relative endpoints of titrations between nickel and SUVs containing DOGS-NTA using a matched pair of samples, one in buffer (outer leaflet accessible) and the other in buffer plus 1% octyl glucoside (all sites accessible). Vesicle-bound signaling complexes were generated in a 75 μL sample volume by incubating vesicles (280 μM in DOGS-NTA- Ni^{2+}) and 30 μM CF in assay buffer for 2 min at 25 $^{\circ}\text{C}$, followed by the addition of CheA (1.2 μM) and CheW (0–35 μM) with gentle vortexing and incubation at 25 $^{\circ}\text{C}$ for 3.5 h.

Vesicle samples were analyzed for signal complex formation by separating the vesicle-bound protein using sedimentation (125 000g for 15 min in a Beckman TLX centrifuge with a TLA-120.2 rotor). Samples of free (supernatant) and total protein (an aliquot removed prior to sedimentation) were analyzed on 15% SDS–polyacrylamide gels (BioWhittaker Molecular Sciences) with software-assisted scanning densitometry (GS-700 Densitometer, Molecular Analyst, version 1.4, Bio-Rad Laboratories).

Enzyme Assays. CheA–CheY phosphotransferase activity was measured in a steady-state coupled spectrophotometric ATPase assay (40, 41) on 2 μL aliquots withdrawn from the samples (incubated for \sim 3.5 h at 25 $^{\circ}\text{C}$). ATPase activities were measured immediately (30 s) after diluting the aliquots 100-fold into buffer with 50 μM CheY and assay reagents (2.5 mM PEP, 4.0 mM ATP, 250 μM β -NADH, and 4 units of PK/LDH enzymes, obtained from Sigma-Aldrich). Specific activities (s^{-1}), defined as the turnover number per mole of CheA subunits in the sample, were determined from the absorbance change at 340 nm ($d[\text{ADP}]/dt = -6220 \text{ dA}_{340}/dt$). The activity of 50 μM CheY samples was subtracted as background. The extent of CheA activation was expressed relative to the activity of 5.0 μM CheA (0.074 s^{-1}), which was regarded as the solution activity of dimeric CheA. Normalized activities (s^{-1}) were computed for each of the samples from the specific activities and the fractions of CheA bound to vesicles.

The ability of CF to act as substrate for CheR was tested using 30 μM CF_{EEEE} incubated with vesicles (1:1 DOPC: DOGS-NTA- Ni^{2+} , 560 μM total lipid). Reactions were initiated by the addition of CheR and SAM at final concentrations of 6 μM and 10 mM, respectively. The 20 μL aliquots were removed at 0.1, 0.5, 2, 3, and 4.5 h, quenched in the course of preparing the samples for SDS–PAGE analysis, and resolved on 12.5% gels. The extent of the CF methylation reaction was estimated by the appearance of a protein band of increased mobility using densitometry, which is a known result of receptor methylation (9).

Curve Fitting. Nonlinear least-squares (NLS) fits of the CheA activity (Act) and vesicle-bound CheA (f_B) data were conducted in Origin version 7.0 (OriginLab Corporation, Northampton, MA) to specific models described in the Results. The parameters were adjusted iteratively in the NLS fitting engine of Origin by the Levenberg–Marquardt method until the errors were minimized (42).

RESULTS

Figure 1 illustrates the scheme used to generate CF/CheW/CheA complexes with the vesicle-templating approach. For simplicity, the CF is depicted in the coiled–coil hairpin dimer arrangement found in the X-ray structure (27) (Figure 1A),

although the extent of CF dimerization in solution and on the surface is not known. CF is depicted to be randomly distributed in solution (Figure 1B) but orients on binding to a vesicle outer surface via the Ni-NTA–histidine interaction, possibly as depicted in Figure 1C. The CF orientation in Figure 1C is consistent with the observation of complete binding to vesicles (>95% of the CF cosediments with vesicles), which reasonably excludes other orientations requiring a larger area per CF molecule bound (i.e., side-on vs end-on binding).² Ternary complexes of CF, CheW, and CheA are then formed on the vesicle surface, and the CheA phosphotransferase activity is measured in the presence of excess CheY in a coupled steady-state ATPase assay (Figure 1D).

Activation of CheA by Surface-Assembled CF. The histogram of CheA activity in Figure 2A shows the effect of surface anchoring on CheA activity. CheA activity is significantly larger in the presence of Ni-NTA-SUVs as compared to samples without vesicles, irrespective of the level of covalent modification on the CF. The trend of increasing the specific activity with increasing levels of covalent modification, which is mimicked by replacing glutamates, E, with glutamines, Q, at the methylation sites (47), has been observed in previous studies of ternary (receptor–CheW–CheA) complexes formed with intact receptor molecules (9–14) and has been attributed to variations in the degree of CheA activation within the complex. The data in Figure 2 are at odds with this interpretation; the trend is eliminated after the activities are normalized to account for the fraction of CheA bound to the vesicle (Figure 2A, right). Instead, these data provide evidence for a receptor–CheW–CheA complex of increasing stability as the level of modification is increased and an activity that remains constant within the complex. Previous studies of kinase activation involving intact receptors have generally not assessed the fraction of CheA bound (9–14); in one instance where it was assessed qualitatively (11), the trend in complex stability as a function of covalent modification agrees with the current observations. A similar increase in stability as a function of the level of covalent modification (from EEEE to QQQQ) was also observed with soluble supramolecular signaling complexes, which were formed using Tar CF fusion proteins (and CheA and CheW) that possess an N-terminal leucine zipper dimerization motif (36, 48).

CheW Dependence of Activation and Binding. The variation in the stability of the signaling complexes is also evident in the CheW dependence of CheA activity (Figure 2B) and vesicle binding (Figure 2C) for signaling complexes made

² The available vesicle surface area per molecule of CF was estimated to be \sim 770 \AA^2 using a value of 11 for the molar ratio of accessible lipid to CF and an area per molecule of 70 \AA^2 for DOPC and DOGS-NTA- Ni^{2+} (43). The molar ratio of accessible lipid to CF was generated using the value of 60% accessibility determined by titration (see Materials and Methods) and the total lipid and protein concentrations in the sample at incubation, 280 μM DOGS-NTA- Ni^{2+} , 280 μM DOPC, and 30 μM CF. The area occupied by a close-packed CF molecule oriented end-on is estimated to be between \sim 330 and \sim 500 \AA^2 , or 2–3 times the cross-sectional area of an α -helix (\sim 165 \AA^2 , refs 44–46) and is expected to result from the two α -helices in the CF coiled–coil hairpin plus unstructured polypeptide at the *c*-terminus. The area required for side-on binding is estimated to be \sim 2500 \AA^2 per CF molecule, in which a CF dimer occupies a rectangle defined by the approximate width (25 \AA) and length (200 \AA) of the dimer (27, 31).

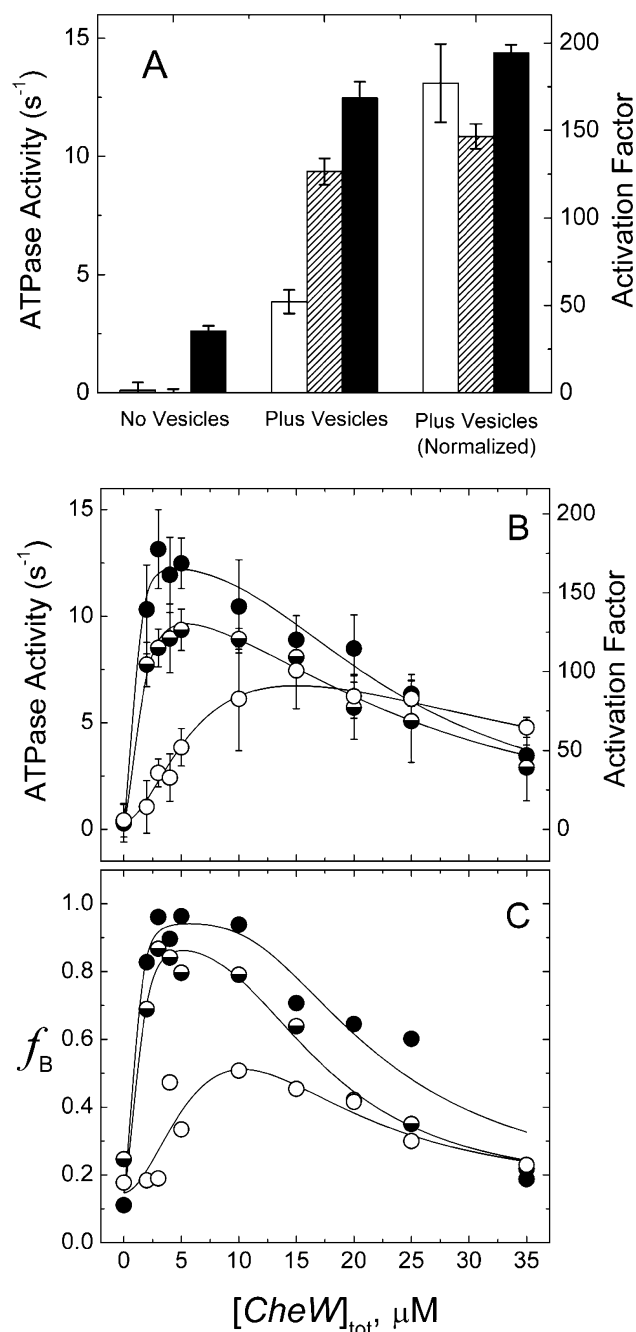
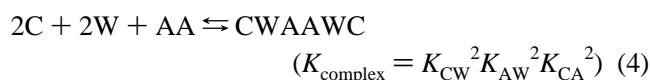
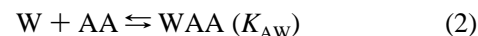


FIGURE 2: CheA activation on vesicle surfaces. (A) Left- and right-hand scales are CheA activity (s^{-1}) and the fold-increase of CheA activity in complexes relative to CheA dimers in solution, respectively. Activities (\pm standard error of three samples) were measured on samples ($1.2 \mu\text{M}$ CheA, $5 \mu\text{M}$ CheW, and $30 \mu\text{M}$ CF) containing CF in low (EEEE), intermediate (QEQE), and high (QQQQ) modification levels (open, striped, and filled bars, respectively) in the absence of SUVs (No Vesicles, left) and with SUVs (Plus Vesicles, middle). The Plus Vesicles (Normalized) data on the right were normalized by the fraction of CheA bound to vesicles, which was determined in parallel by sedimentation. Normalized activities represent the averages of six samples (\pm standard error), determined at different CheW concentrations (3, 4, 5, 10, 15, and 20 μM). (B) The activity of CheA as a function of the total CheW concentration $[\text{CheW}]_{\text{tot}}$ and vesicle-templated CF in different modification states (EEEE, \circ ; QEQE, \ominus ; and QQQQ, \bullet), prepared as described in the Materials and Methods. Each point is an average of three samples (\pm standard deviation). (C) The fraction CheA of bound to vesicle-templated CF (f_B) as a function of $[\text{CheW}]_{\text{tot}}$, for CF in the three modification states (symbols as in panel B). The curves in panels B and C represent fits of the data generated as described in the text.

with CFs in the different modification states (EEEE, QEQE, and QQQQ). The rise and fall in activity and binding are consistent with the known properties of CheW, which binds both to CheA and to the receptor cytoplasmic domain (6, 49). Initially, CheW facilitates an increase in the phosphotransferase and vesicle binding activities through a CF–CheW–CheA bridging interaction. Increasing the CheW concentration further leads to saturation of the binding sites on CheA and CF, and consequently, the CheA enzyme and vesicle binding activities both lessen. The relative stabilities of the CF/CheW/CheA complexes are apparent in the maximum values for activity and binding and the CheW concentrations at which these maxima occur. The CF_{QQQQ}-containing complex is judged to be most stable since it has the largest maximum values of CheA activity and binding ($f_B \sim 0.95$) at the smallest CheW concentration ($< 5 \mu\text{M}$). The CF_{EEEE}-containing complex is the least stable, which is reflected in the smaller maximum values of activity and f_B ($\sim 50\%$ of CF_{QQQQ} complexes) and the significantly larger CheW concentration at which the maximum is observed ($\sim 12 \mu\text{M}$).

A model for complex formation, which assumes that the CheA activity is proportional to the fraction of CheA in signaling complexes bound to vesicles, f_B , captures the salient features of these data and provides preliminary estimates of the relative stability of signaling complexes as a function of covalent modification. The model is based on pairwise associations between CF (C), CheW (W), and CheA dimers (AA) according to equilibrium expressions (eqs 1–4), mass conservation relationships (eqs 5–7), and expressions for the fraction of CheA bound to vesicles (f_B , eq 8) and CheA activity (Act, eq 9). In eq 9, Act_0 and Act_{Max} are the background and maximum (100% CheA-bound) activities, respectively.



$$[\text{C}]_{\text{tot}} = [\text{C}] + [\text{CW}] + 2[\text{CWAAWC}] \quad (5)$$

$$[\text{W}]_{\text{tot}} = [\text{W}] + [\text{AAW}] + 2[\text{WAAW}] + 2[\text{CWAAWC}] \quad (6)$$

$$[\text{AA}]_{\text{tot}} = [\text{AA}] + [\text{AAW}] + [\text{WAAW}] + [\text{CWAAWC}] \quad (7)$$

$$f_B = \frac{[\text{CWAAWC}]}{([\text{AA}] + [\text{WAA}] + [\text{WAAW}] + [\text{CWAAWC}])} \quad (8)$$

$$\text{Act} = \text{Act}_0 + f_B \text{Act}_{\text{Max}} \quad (9)$$

The constraints and assumptions of this model were chosen to be consistent with the experimental conditions and observations: (i) CheA was assumed to be present only as a dimer since the total CheA concentration in the samples was about 3-fold larger than the dissociation constant for

Table 1: Normalized CheA Activity and CheA and CheW Bound Fractions to Vesicles Presenting Wild-Type CFs^a

modification level	phosphotransferase activity s ⁻¹ (per mol CheA bound)	fold activation ^b	f _B (CheA)	f _B (CheW)
EEEE	15.7 ± 1.6	212 ± 22	0.59 ± 0.04	0.37 ± 0.03
QEQE	10.9 ± 0.4	147 ± 5	0.83 ± 0.01	0.64 ± 0.02
QQQQ	13.2 ± 0.3	178 ± 4	0.93 ± 0.01	0.87 ± 0.01

^a Averages and uncertainties (standard errors of the mean) were calculated from triplicate samples. Sample compositions were 30 μM CF, 560 μM total lipid (1:1 DOPC:DOGS-NTA-Ni²⁺) in the form of SUVs, 1.2 μM CheA, and either 5 μM (CF_{QQQQ} and CF_{QEQE}) or 15 μM (CF_{EEEE}) CheW.

^b Fold activations were determined by dividing the normalized activities of CF/CheW/CheA complexes by the solution activity of 5.0 μM CheA (0.074 s⁻¹).

CheA dimerization (39, 40). (ii) Direct interaction between CF and CheA was neglected in the absence of CheW since CheA exhibited small levels of binding to vesicle-templated CF in the absence of CheW (Figure 2C). (iii) The approximate proportionality between activity and f_B versus [W] data was interpreted to be consistent with a single surface-active species (CWAAWC).

The values for [AA]_{tot}, [W]_{tot}, and [C]_{tot} were shared among the three sets of data (CF_{QQQQ}, CF_{QEQE}, and CF_{EEEE}) in the fits of the Act and f_B versus [W]_{tot} data (Figure 2B and 2C, respectively). [AA]_{tot} was fixed to the molar concentration of CheA dimer used in the experiments (0.6 μM). Act_{Max} was set to the average normalized activity (13.5 s⁻¹) observed for all three levels of modification (Figure 2A and Table 1). Act₀ was permitted to adjust in the fits, as were the individual values of the association constants. [C]_{tot} was fixed to a value (10 μM) that corresponded to the CheW binding capacity of 30 μM vesicle-bound CF, which was determined in preliminary binding experiments (data not shown). A systematic analysis of the influence of [C]_{tot} on the fit parameters revealed that the relative complex stabilities (e.g., K_{complex}(QQQQ)/K_{complex}(EEEE)) were relatively insensitive to the assigned value of [C]_{tot} over a range of 10–30 μM, but the absolute values of these parameters varied.

Fits of the activity data in Figure 2B by the model and constraints described previously resulted in values for K_{complex} of 1.3, 0.09, and 0.002 μM⁻⁴ for complexes formed with CF_{QQQQ}, CF_{QEQE}, and CF_{EEEE}, respectively, and a value for Act₀ of 0.36 ± 0.14 s⁻¹. Fits to the CheW dependence of CheA binding data (Figure 2C) generated estimates for K_{complex} of 4.6, 1.0, and 0.014 μM⁻⁴ in CF_{QQQQ}, CF_{QEQE}, and CF_{EEEE}-containing complexes, respectively. The differences in the absolute values of K_{complex} obtained from binding data, versus the estimates obtained from the activities, may illustrate in part the dependency of these parameters on the details of the model (e.g., the values chosen for [C]_{tot} and Act_{Max}), which prevents useful comparisons between the absolute values of model-derived estimates for the CheA–CheW and CheW–receptor interaction constants and the measured values until the properties of vesicle-templated CFs are fully characterized. The complexity inherent in the system, including the presence of soluble and surface-bound species and possible contributions from multivalent interactions, also presents challenges for making such absolute comparisons. Nonetheless, the significant trend in K_{complex}, which is similar in both sets of estimates (> 100-fold), reflects the change in stability of signaling complexes as a function of covalent modification. The results of a similar analysis conducted with a simpler model, in which only monovalent C–W and W–A interactions were considered to contribute to the formation of a CWA complex, also produced a

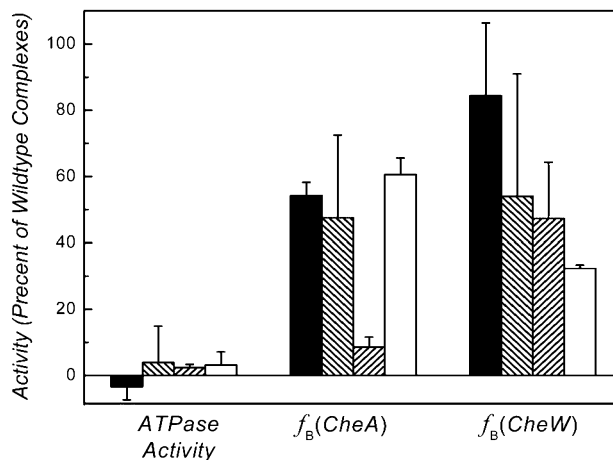


FIGURE 3: Effects of CF mutations on activity and binding. Activities and f_B are expressed as percentages relative to the complexes containing wild-type CF under the same conditions (Table 1) for the *lock-off* mutant CF:S461L (in the QEQE level of covalent modification, black bars) and the *tod* mutants CF:E383A and CF:E382P (the EEEE and QQQQ forms of CF:E383A are represented by left- and right-slanting striped bars, respectively; the QEQE form of CF:E382P is represented by open bars). Uncertainties are error-propagated values using standard errors of the mean determined on triplicate samples with the wild type and mutant complexes.

significant trend (~100-fold) in the values of the constant of formation for the complex.

Signaling Mutations in the CF Affect CheA and CheW Binding to Various Extents. Vesicle-templated CFs are functionally similar to intact receptors in the absence of (attractant) ligand since the cytoplasmic domains activate CheA in both situations. We obtained evidence that this functional similarity is based on a common structural organization from an analysis of a limited number of *lock-off* and trimer-of-dimer (*tod*) mutations (23, 50), which are located in the cytoplasmic domain at the positions shown in Figure 1. *Lock-off* mutations mimic attractant-bound ternary complexes by producing complexes that are inactive in the absence of ligand (50, 51). The *lock-off* allele, a serine-461 to leucine (S461L) mutation in the intact Tar protein, is located close to the sites of methylation. The *tod* mutations, which are known to disrupt the trimer-of-dimer interaction in the homologous Tsr protein (23), are located near the turn in the coiled-coil hairpin. The two alleles tested correspond to the point mutations E383A and E382P in Tar. CheA and CheW binding, and also CheA activation, were measured using vesicle-templated CFs. CheA activation (Figure 3) was reduced significantly by all of these mutations, but CheA and CheW binding were retained to varying degrees, relative to wild-type CFs in the corresponding level of covalent modification (Table 1). The *lock-off* S461L CF (QEQE)

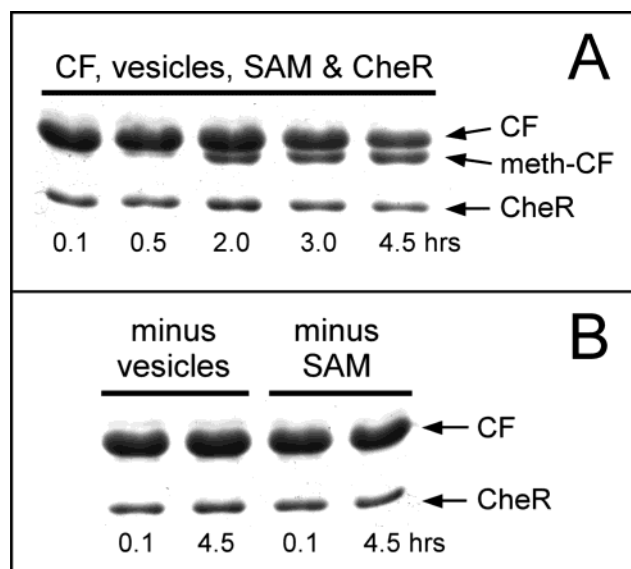


FIGURE 4: CheR-catalyzed methylation of vesicle-templated CF. (A) The change in electrophoretic mobility of methylated CF indicates the reaction progress in a sample containing CF_{EEEE}, vesicles, SAM, and CheR (~35% at 4.5 h). (B) Minus vesicle and minus SAM controls.

retained substantial binding strength overall, which is consistent with the known ability of *lock-off* mutant receptors to compete for a limited pool of CheA and CheW in mixtures with activating receptors (51). The lower amounts of CheA and/or CheW binding exhibited by CFs containing *tod* mutations is consistent in the disrupting effect that these types of mutations can have on the formation of receptor patches in vivo (23). The interference with kinase activation by the *tod* mutations is evidence that trimer-of-dimer-like interactions are also present in the vesicle-templated CFs and are necessary for CheA activation.

Surface-Assembly Enhances CF Methyl-Accepting Activity. The adaptation branch in the chemotaxis pathway involves reversible receptor methylation and demethylation, which are catalyzed by a methyltransferase and a methylesterase, respectively (26). Receptor methylation is a result of methyl group transfer from *s*-adenosyl-L-methionine (SAM) to specific glutamic acid residues in the cytoplasmic domain of MCPs (52–54). The process of methylation has been demonstrated to occur, at least in part, by a mechanism that involves transmethylation in which the transferase binds to the cytoplasmic domain through a tethering interaction and catalyzes methyl group transfer on a cytoplasmic domain of an adjacent receptor subunit through active site–substrate site interactions (19–21).

Surface-assembled CF can be expected to generate the close associations between cytoplasmic domains that are needed for efficient methylation via a trans mechanism. The role of surface-assembly in promoting efficient CF methylation was assessed by comparing the extent of methylation of CF on vesicle surfaces relative to CF in solution. The data in Figure 4 demonstrated that binding to the vesicle surface enhanced CF substrate activity significantly. The SDS–polyacrylamide gels in Figure 4A showed that only in the presence of vesicles, SAM, and transferase did the CF convert to a more rapidly migrating band corresponding to methylated protein. The faster migrating band was not observed in the vesicle-minus and SAM-minus controls

(Figure 4B), which demonstrated that vesicle binding was required for substrate activity and that the more rapidly migrating band was not due to proteolysis of the CF, respectively. The requirement of vesicle-templating for efficient methyl group incorporation was verified by scintillation counting using tritiated SAM as the methyl group donor (data not shown).

DISCUSSION

The polyhistidine tag has found widespread use as a convenient and effective genetically encoded affinity tag for protein purification and screening applications, through the interaction of the histidine tag with metal–chelator complexes such as nickel–nitrilotriacetic acid (55–57). The histidine tag–Ni–NTA interaction has also been used in biosensor applications (56–59) and as a method for generating 2-D protein crystals when the Ni–NTA moiety is present as a headgroup in lipid monolayers (38, 60–62). This latter use inspired us to consider it as a means to restore the functional properties of membrane-associated proteins. The results described above demonstrate the significant effect that binding receptor fragments to vesicle surfaces can have in restoring biochemical activity. Complexes of transmembrane receptors, membrane-associated adaptor proteins, and cytoplasmic enzymes are a ubiquitous feature of signaling cascades (3–5). The architecture of these complexes and their rates of assembly and disassembly are key to understanding the regulation of these biochemical processes. The vesicle-templating approach presented here should prove to be useful in such studies.

The application of this method to the bacterial chemotaxis system restores both the kinase activating and the methyl-accepting properties to the CF. On the basis of these observations, we conclude that binding to the vesicle surface promotes a lateral organization among CF subunits that resembles the organization of cytoplasmic domains in receptor-containing membranes. This conclusion is supported by the similar effects that *lock-off* and *tod* point mutations produce in templated CF and intact receptors and suggests that inter-dimer interactions (e.g., a trimer-of-dimer organization (23, 27)) are critical for kinase activation. Also, the mutations appear to generate the kinase-inactive phenotype through different mechanisms, either by producing inactive complexes or by disrupting complex formation. The CF with the *lock-off* mutation retains significant CheA and CheW binding affinity while forming inactive signaling complexes; CFs with the *tod* mutations form inactive complexes at the expense of the protein–protein interaction strength to varying degrees.

The CheA activity and binding data generated with the vesicle-templated CF system demonstrate that signaling complex stability can be strongly influenced by covalent modification, and the preliminary analysis by a pairwise binding model supports this conclusion. The correlations between complex stability, CheA activation, and covalent modification in our data are consistent with previous studies of kinase activation conducted with intact receptors, which report negligible CheA activation in the lowest covalent modification level and dramatic increases as the modification is increased (9–14). These studies, which began with the ground-breaking work of Simon et al. (9), have been

typically conducted at relatively low concentrations of CheW (0.5–2.0 μM) and CheA (0.1–1.0 μM); concentrations that correspond to the portion of our data where the differences in CheA activity and binding between lowest and highest level of covalent modification are the greatest (Figure 2B,C; $[\text{W}]_{\text{tot}} = 2 \mu\text{M}$). This variation in complex stability may prove to be a significant factor in regulating kinase activity in the cell, since bacteria like *E. coli* integrate the effects of the different chemoeffector concentrations through a set of homologous receptors (15). CheA is the sole protein in *E. coli* through which these chemotactic responses are mediated. Therefore, regulating the extent of CheA association with (and activation by) receptors via covalent modification provides a means to weigh the response to the various chemoeffectors, which can be present simultaneously at vastly different concentrations.

ACKNOWLEDGMENT

We thank Frances Antommattei for assistance in site-directed mutagenesis of the CF, Abdalin Asinas and Tatiana Besschetnova for preparing *tod* mutants, Li Zhi for assistance with the ATPase assay, Laila Kott for purified CheW protein, and Bill Vining and Nicholas Fisher for assistance with Figure 1 artwork.

REFERENCES

- Singer, S. J., and Nicholson, G. L. (1972) *Science* 175, 720–731.
- Brandts, J. F., and Jacobson, B. S. (1983) *Surv. Synth. Pathol. Res.* 2, 107–114.
- Pawson, T., and Nash, P. (2003) *Science* 300, 445–452.
- Jordan, M. S., Singer, A. L., and Koretzky, G. A. (2003) *Nat. Immunol.* 4, 110–116.
- Sheng, M., and Sala, C. (2001) *Annu. Rev. Neurosci.* 24, 1–29.
- Gegner, J. A., Graham, D. R., Roth, A. F., and Dahlquist, F. W. (1992) *Cell* 70, 975–982.
- Schuster, S. C., Swanson, R. V., Alex, L. A., Bourret, R. B., and Simon, M. I. (1993) *Nature* 365, 343–347.
- Borkovich, K. A., Kaplan, N., Hess, J. F., and Simon, M. I. (1989) *Proc. Natl. Acad. Sci. U.S.A.* 86, 1208–1212.
- Borkovich, K. A., Alex, L. A., and Simon, M. I. (1992) *Proc. Natl. Acad. Sci. U.S.A.* 89, 6756–6760.
- Barnakov, A. N., Barnakova, L. A., and Hazelbauer, G. L. (1998) *J. Bacteriol.* 180, 6713–6718.
- Li, G., and Weis, R. M. (2000) *Cell* 100, 357–365.
- Bornhorst, J. A., and Falke, J. J. (2000) *Biochemistry* 39, 9486–9493.
- Levit, M. N., and Stock, J. B. (2002) *J. Biol. Chem.* 277, 36760–36765.
- Bornhorst, J. A., and Falke, J. J. (2003) *J. Mol. Biol.* 326, 1597–1614.
- Adler, J. (1975) *Annu. Rev. Biochem.* 44, 341–356.
- Maddock, J. R., and Shapiro, L. (1993) *Science* 259, 1717–1723.
- Sourjik, V., and Berg, H. C. (2000) *Mol. Microbiol.* 37, 740–751.
- Cantwell, B. J., Draheim, R. R., Weart, R. B., Nguyen, C., Stewart, R. C., and Manson, M. D. (2003) *J. Bacteriol.* 185, 2354–2361.
- Wu, J., Li, J., Li, G., Long, D. G., and Weis, R. M. (1996) *Biochemistry* 35, 4984–4993.
- Li, J., Li, G., and Weis, R. M. (1997) *Biochemistry* 36, 11851–11857.
- Le Moual, H., Quang, T., and Koshland, D. E., Jr. (1997) *Biochemistry* 36, 13441–13448.
- Gestwicki, J. E., and Kiessling, L. L. (2002) *Nature* 415, 81–84.
- Ames, P., Studdert, C. A., Reiser, R. H., and Parkinson, J. S. (2002) *Proc. Natl. Acad. Sci. U.S.A.* 99, 7060–7065.
- Le Moual, H., and Koshland, D. E., Jr. (1996) *J. Mol. Biol.* 261, 568–585.
- Zhulin, I. B. (2001) *Adv. Microbiol. Physiol.* 45, 157–198.
- Springer, M. S., Goy, M. F., and Adler, J. (1979) *Nature* 280, 279–284.
- Kim, K. K., Yokota, H., and Kim, S.-H. (1999) *Nature* 400, 787–792.
- Milburn, M. V., Privé, G. G., Milligan, D. L., Scott, W. G., Yeh, J., Jancarik, J., Koshland, D. E., Jr., and Kim, S.-H. (1991) *Science* 254, 1342–1347.
- Yeh, J. I., Biemann, H. P., Privé, G. G., Pandit, J., Koshland, D. E., Jr., and Kim, S.-H. (1996) *J. Mol. Biol.* 262, 186–201.
- Falke, J. J., Bass, R. B., Butler, S. L., Chervitz, S. A., and Danielson, M. A. (1997) *Annu. Rev. Cell Dev. Biol.* 13, 457–512.
- Weis, R. M., Hirai, T., Chalah, A., Kessel, M., Peters, P. J., and Subramaniam, S. (2003) *J. Bacteriol.* 185, 3636–3643.
- Ninfa, E. G., Stock, A., Mowbray, S., and Stock, J. (1991) *J. Biol. Chem.* 266, 9764–9770.
- Bogonez, E., and Koshland, D. E., Jr. (1985) *Proc. Natl. Acad. Sci. U.S.A.* 82, 4891–4895.
- Ames, P., and Parkinson, J. S. (1994) *J. Bacteriol.* 176, 6340–6348.
- Cochran, A. G., and Kim, P. S. (1996) *Science* 271, 1113–1116.
- Liu, Y., Levit, M., Lurz, R., Surette, M. G., and Stock, J. B. (1997) *EMBO J.* 16, 7231–7240.
- Francis, N. R., Levit, M. N., Shaikh, T. R., Melanson, L. A., Stock, J. B., and DeRosier, D. J. (2002) *J. Biol. Chem.* 277, 36755–36759.
- Schmitt, L., Dietrich, L., and Tampé, R. J. (1994) *J. Am. Chem. Soc.* 116, 8485–8491.
- Kott, L., Braswell, E. M., Shroud, A. L., and Weis, R. M. (2003) *Biochim. Biophys. Acta*, in press.
- Surette, M. G., Levit, M., Liu, Y., Lukat, G., Ninfa, E. G., Ninfa, A., and Stock, J. B. (1996) *J. Biol. Chem.* 271, 939–945.
- Norby, J. G. (1988) *Methods Enzymol.* 156, 116–119.
- Press, W. H., Flannery, B. P., Teukolsky, S. A., and Vetterling, W. T. (1986) *Numerical Recipes. The Art of Scientific Computing*, pp 523–528, Cambridge University Press, Cambridge.
- Nagle, J. F., and Tristram-Nagle, S. (2000) *Biochim. Biophys. Acta* 1469, 159–195.
- Luecke, H., Schobert, B., Richter, H. T., Cartailler, J. P., and Lanyi, J. K. (1999) *J. Mol. Biol.* 291, 899–911.
- Ren, G., Reddy, V. S., Cheng, A., Melnyk, P., and Mitra, A. K. (2001) *Proc. Natl. Acad. Sci. U.S.A.* 98, 1398–1403.
- Heymann, J. A. W., Sarker, R., Hirai, T., Shi, D., Milne, J. L. S., Maloney, P. C., and Subramaniam, S. (2000) *EMBO J.* 20, 4408–4413.
- Dunten, P., and Koshland, D. E., Jr. (1991) *J. Biol. Chem.* 266, 1491–1496.
- Levit, M. N., Liu, Y., and Stock, J. B. (1999) *Biochemistry* 38, 6651–6658.
- Boukhvalova, M. S., Dahlquist, F. W., and Stewart, R. C. (2002) *J. Biol. Chem.* 277, 22251–22259.
- Mutoh, N., Oosawa, K., and Simon, M. I. (1986) *J. Bacteriol.* 167, 992–998.
- Borkovich, K. A., and Simon, M. I. (1990) *Cell* 63, 1339–1348.
- Kehry, M. R., and Dahlquist, F. W. (1982) *J. Biol. Chem.* 257, 378–386.
- Terwilliger, T. C., and Koshland, D. E., Jr. (1984) *J. Biol. Chem.* 259, 7719–7725.
- Kehry, M. R., Engstrom, P., Dahlquist, F. W., and Hazelbauer, G. L. (1983) *J. Biol. Chem.* 258, 5050–5055.
- Crowe, J., Doherty, H., Gentz, R., Hochuli, E., Stuber, D., and Henco, K. (1994) *Methods Mol. Biol.* 31, 371–387.
- Jones, C., Patel, A., Griffin, S., Martin, J., Young, P., O'Donnell, K., Silverman, C., Porter, T., and Chaiken, I. (1995) *J. Chromatogr., A* 707, 3–22.
- Terpe, K. (2003) *Appl. Microbiol. Biotechnol.* 60, 523–533.
- Nieba, L., Nieba-Axmann, S. E., Persson, A., Hamalainen, M., Edebratt, F., Hansson, A., Lidholm, J., Magnusson, K., Karlsson, A. F., and Pluckthun, A. (1997) *Anal. Biochem.* 252, 217–228.
- Gershon, P. D., and Khilko, S. (1995) *J. Immunol. Methods* 183, 65–76.
- Frey, W., Schief, W. R., Jr., Pack, D. W., Chen, C. T., Chilkoti, A., Stayton, P., Vogel, V., and Arnold, F. H. (1996) *Proc. Natl. Acad. Sci. U.S.A.* 93, 4937–4941.
- Celia, H., Wilson-Kubalek, E., Milligan, R. A., and Teyton, L. (1999) *Proc. Natl. Acad. Sci. U.S.A.* 96, 5634–5639.
- Thess, A., Hutschenreiter, S., Hofmann, M., Tampé, R., Baumeister, W., and Guckenberger, R. (2002) *J. Biol. Chem.* 277, 36321–36328.

Name: _____ Block: _____

Scientific Notation/Significant Figures Key

1. Convert each of the following into scientific notation.

- | | |
|-------------------------|---------------------------|
| a) 3427 | j) 0.0000455 |
| b) 0.00456 | k) 2205.2 |
| c) 123,453 | l) 0.982×10^{-3} |
| d) 172 | m) 0.0473 |
| e) 0.000984 | n) 650,502 |
| f) 0.502 | o) 3.03×10^{-1} |
| g) 3100.0×10^2 | p) 20.4×10^5 |
| h) 0.0114×10^4 | q) 1000×10^{-3} |
| i) 107.2 | |

2. Determine the number of significant figures in each of the following:

- | | | |
|-------------|-------------------------|---------------------------|
| a) 3427 | g) 3100.0×10^2 | l) 0.982×10^{-3} |
| b) 0.00456 | h) 0.0114×10^4 | m) 0.0473 |
| c) 123,453 | i) 107.2 | n) 650,502 |
| d) 172 | j) 0.0000455 | o) 3.03×10^{-1} |
| e) 0.000984 | k) 2205.2 | p) 20.4×10^5 |
| f) 0.502 | | |

3. Convert each into decimal form.

- | | |
|--------------------------|---------------------------|
| a) 1.56×10^4 | e) 0.00259×10^5 |
| b) 0.56×10^{-2} | f) 13.69×10^{-2} |
| c) 3.69×10^{-2} | g) 6.9×10^4 |
| d) 736.9×10^5 | |

4. Calculate the following. Give the answer in correct scientific notation.

a) $\frac{3.95 \times 10^2}{1.5 \times 10^6}$

b) $\frac{4.44 \times 10^7}{2.25 \times 10^5}$

c) $\frac{1.05 \times 10^{-26}}{4.2 \times 10^{56}}$

d) $\frac{6.022 \times 10^{23}}{3.011 \times 10^{-56}}$

e) $(3.5 \times 10^2)(6.45 \times 10^{10})$

f) $(4.50 \times 10^{-12})(3.67 \times 10^{-12})$

g) $(2.5 \times 10^9)(6.45 \times 10^4)$

h) $(6.88 \times 10^2)(3.45 \times 10^{-10})$

5. Round each of the following to 3 significant figures.

a) 77.0653

b) 0.00023350

c) 10.2030

d) 2.895×10^{21}

6. Calculate the answer, use the correct number of significant figures.

a) $(0.32)(14.50)(120) =$

b) $(24.1)/(0.005) =$

c) $(3.9)(6.05)(420) =$

d) $(14.1)/5 =$

Common Lab Safety signs you must know – see book and run some searches online for common lab safety symbols and signs. Sometimes you will see a different presentation of one of these signs – study them. Also, please read (and reread) all the safety rules handed out on the first day of class.



MATERIAL SAFETY DATA SHEET

Date Printed: 08/26/2009

Date Updated: 01/16/2009

Version 1.6

Section 1 - Product and Company Information

Product Name	DIMETHYLMERCURY, 95%
Product Number	328081
Brand	ALDRICH
Company	Sigma-Aldrich
Address	3050 Spruce Street SAINT LOUIS MO 63103 US
Technical Phone:	800-325-5832
Fax:	800-325-5052
Emergency Phone:	314-776-6555

Section 2 - Composition/Information on Ingredient

Substance Name	CAS #	SARA 313
DIMETHYLMERCURY	593-74-8	Yes

Formula	C2H6Hg
Synonyms	Dimethyl mercury * Methyl mercury
RTECS Number:	OW3010000

Section 3 - Hazards Identification

EMERGENCY OVERVIEW

Flammable (USA) Highly Flammable (EU). Highly Toxic (USA) Very Toxic (EU). Dangerous for the environment.
Very toxic by inhalation, in contact with skin and if swallowed.
Danger of cumulative effects. Irritating to eyes, respiratory system and skin. Very toxic to aquatic organisms, may cause long-term adverse effects in the aquatic environment.
Neurological hazard. Target organ(s): Kidneys. Calif. Prop. 65 developmental hazard.

HMIS RATING

HEALTH: 3
FLAMMABILITY: 3
REACTIVITY: 0

NFPA RATING

HEALTH: 3
FLAMMABILITY: 3
REACTIVITY: 0

For additional information on toxicity, please refer to Section 11.

Section 4 - First Aid Measures

ORAL EXPOSURE

If swallowed, wash out mouth with water provided person is conscious. Call a physician immediately.

INHALATION EXPOSURE

If inhaled, remove to fresh air. If not breathing give artificial respiration. If breathing is difficult, give oxygen.

DERMAL EXPOSURE

In case of skin contact, flush with copious amounts of water for at least 15 minutes. Remove contaminated clothing and shoes. Call a physician.

EYE EXPOSURE

In case of contact with eyes, flush with copious amounts of water for at least 15 minutes. Assure adequate flushing by separating the eyelids with fingers. Call a physician.

Section 5 - Fire Fighting Measures

FLAMMABLE HAZARDS

Flammable Hazards: Yes

EXPLOSION HAZARDS

Vapor may travel considerable distance to source of ignition and flash back. Container explosion may occur under fire conditions.

FLASH POINT

41 °F 5 °C Method: closed cup

AUTOIGNITION TEMP

N/A

FLAMMABILITY

N/A

EXTINGUISHING MEDIA

Suitable: Water spray. Carbon dioxide, dry chemical powder, or appropriate foam.

FIREFIGHTING

Protective Equipment: Wear self-contained breathing apparatus and protective clothing to prevent contact with skin and eyes. Specific Hazard(s): Flammable liquid. Emits toxic fumes under fire conditions.

Section 6 - Accidental Release Measures

PROCEDURE TO BE FOLLOWED IN CASE OF LEAK OR SPILL

Evacuate area. Shut off all sources of ignition.

PROCEDURE(S) OF PERSONAL PRECAUTION(S)

Wear self-contained breathing apparatus, rubber boots, and heavy rubber gloves.

METHODS FOR CLEANING UP

Cover with dry-lime, sand, or soda ash. Place in covered containers using non-sparking tools and transport outdoors. Ventilate area and wash spill site after material pickup is complete.

Section 7 - Handling and Storage

HANDLING

User Exposure: Do not breathe vapor. Do not get in eyes, on skin, on clothing. Avoid prolonged or repeated exposure.

STORAGE

Suitable: Keep tightly closed. Keep away from heat, sparks, and open flame.

Section 8 - Exposure Controls / PPE

ENGINEERING CONTROLS

Safety shower and eye bath. Use nonsparking tools. Use only in a chemical fume hood.

PERSONAL PROTECTIVE EQUIPMENT

Respiratory: Use respirators and components tested and approved under appropriate government standards such as NIOSH (US) or CEN (EU). Where risk assessment shows air-purifying respirators are appropriate use a full-face respirator with multi-purpose combination (US) or type ABEK (EN 14387) respirator cartridges as a backup to engineering controls. If the respirator is the sole means of protection, use a full-face supplied air respirator.
Hand: Highly resistant laminate gloves under a long-cuffed neoprene or nitrile glove.
Eye: Chemical safety goggles.

GENERAL HYGIENE MEASURES

Wash contaminated clothing before reuse. Wash thoroughly after handling.

EXPOSURE LIMITS, RTECS

Country	Source	Type	Value
USA	ACGIH	TWA	0.01
		STEL	0.03 MG/M3
Remarks: Skin			
USA	MSHA Standard-air	TWA	0.001 PPM (0.01 MG(HG)/M3)
USA	OSHA.	PEL	8H TWA 0.01 MG(HG)/M3
New Zealand OEL			
Remarks: check ACGIH TLV			

Section 9 - Physical/Chemical Properties

Appearance	Physical State: Liquid	
Property	Value	At Temperature or Pressure
Molecular Weight	230.66 AMU	
pH	N/A	
BP/BP Range	91.0 - 92.0 °C	
MP/MP Range	- 43.0 °C	
Freezing Point	N/A	
Vapor Pressure	N/A	
Vapor Density	N/A	
Saturated Vapor Conc.	N/A	
SG/Density	3.19 g/cm3	
Bulk Density	N/A	
Odor Threshold	N/A	
Volatile%	N/A	
VOC Content	N/A	
Water Content	N/A	
Solvent Content	N/A	
Evaporation Rate	N/A	
Viscosity	N/A	
Surface Tension	N/A	
Partition Coefficient	N/A	
Decomposition Temp.	N/A	

Flash Point	41 °F 5 °C	Method: closed cup
Explosion Limits	N/A	
Flammability	N/A	
Autoignition Temp	N/A	
Refractive Index	1.543	
Optical Rotation	N/A	
Miscellaneous Data	N/A	
Solubility	N/A	

N/A = not available

Section 10 - Stability and Reactivity

STABILITY

Stable: Stable.

Materials to Avoid: Strong oxidizing agents.

HAZARDOUS DECOMPOSITION PRODUCTS

Hazardous Decomposition Products: Carbon monoxide, Carbon dioxide
Mercury/mercury oxides.

HAZARDOUS POLYMERIZATION

Hazardous Polymerization: Will not occur

Section 11 - Toxicological Information

ROUTE OF EXPOSURE

Skin Contact: Causes skin irritation.

Skin Absorption: Readily absorbed through skin. May be fatal if absorbed through skin.

Eye Contact: Causes eye irritation.

Inhalation: Material is irritating to mucous membranes and upper respiratory tract. May be fatal if inhaled.

Ingestion: May be fatal if swallowed.

TARGET ORGAN(S) OR SYSTEM(S)

Nerves. Kidneys.

SIGNS AND SYMPTOMS OF EXPOSURE

To the best of our knowledge, the chemical, physical, and toxicological properties have not been thoroughly investigated. In contrast to inorganic mercury compounds, alkyl mercury compounds rapidly pass through the placenta and blood brain barrier. The peripheral and central nervous systems and the kidney are major target organs. Methylmercury poisoning symptoms result primarily from damage to the nervous system. The symptoms are primarily characterized by loss of sensation in the hands and feet and in areas around the mouth, diminution of vision resulting in tunnel vision, ataxia, dysarthria, and hearing loss. Severe poisoning produces blindness, coma and death. There is a latent period of weeks to months before development of the poisoning symptoms. Mercury shows a specificity to damage small nerve cells in the cerebellum and visual cortex. Methylmercury causes degeneration and necrosis of neurons in the focal areas of the cerebral cortex, especially within the visual areas of the occipital cortex and the granular layer of the cerebellum. It has been found that methylmercury inhibits protein synthesis in the brain before symptoms of poisoning appear and that recovery of protein synthesis does not occur in granular cells as it does recover in other neuronal cell types. Consumption by pregnant women has caused serious neurological disorders in their offspring resulting in mental retardation with cerebral

palsy. Acute exposure to nonlethal levels of methylmercury results in

CONDITIONS AGGRAVATED BY EXPOSURE

May cause nervous system disturbances.

IARC CARCINOGEN LIST

Rating: Group 2B

CHRONIC EXPOSURE - TERATOGEN

Result: May cause congenital malformation in the fetus.

CHRONIC EXPOSURE - MUTAGEN

Species: Human
Dose: 20 MG/L
Cell Type: lymphocyte
Mutation test: DNA damage

Species: Human
Dose: 43400 NMOL/L
Cell Type: lymphocyte
Mutation test: Cytogenetic analysis

Species: Human
Dose: 1730 NMOL/L
Cell Type: lymphocyte
Mutation test: SLN

Species: Rat
Dose: 20 MG/L
Cell Type: lymphocyte
Mutation test: DNA damage

Species: Rat
Dose: 20 MG/L
Cell Type: Other cell types
Mutation test: DNA damage

Species: Mouse
Dose: 25 MG/L
Cell Type: Other cell types
Mutation test: Other mutation test systems

Species: Hamster
Dose: 40 MG/L
Cell Type: ovary
Mutation test: Cytogenetic analysis

Section 12 - Ecological Information

No data available.

Section 13 - Disposal Considerations

APPROPRIATE METHOD OF DISPOSAL OF SUBSTANCE OR PREPARATION

Contact a licensed professional waste disposal service to dispose of this material. Observe all federal, state, and local environmental regulations.

Section 14 - Transport Information

DOT

Proper Shipping Name: Toxic by inhalation liquid,
flammable, n.o.s.
UN#: 3383
Class: 6.1
Packing Group: Packing Group I
Hazard Label: Poison inhalation hazard
Hazard Label: Flammable liquid
PIH: Zone A

IATA

Proper Shipping Name: Toxic by inhalation liquid,
flammable, n.o.s.
IATA UN Number: 3383
Hazard Class: 6.1
Packing Group: I
Not Allowed - Aircraft: Not permitted for air
transport.

Section 15 - Regulatory Information

EU DIRECTIVES CLASSIFICATION

Symbol of Danger: T+-N
Indication of Danger: Very toxic. Dangerous for the environment.
R: 26/27/28-33-50/53
Risk Statements: Very toxic by inhalation, in contact with skin
and if swallowed. Danger of cumulative effects. Very toxic to
aquatic organisms, may cause long-term adverse effects in the
aquatic environment.
S: 13-28-36-45-60-61
Safety Statements: Keep away from food, drink, and animal
feedingstuffs. After contact with skin, wash immediately with
plenty of soap-suds. Wear suitable protective clothing. In case
of accident or if you feel unwell, seek medical advice
immediately (show the label where possible). This material and
its container must be disposed of as hazardous waste. Avoid
release to the environment. Refer to special instructions/safety
data sheets.

US CLASSIFICATION AND LABEL TEXT

Indication of Danger: Flammable (USA) Highly Flammable (EU).
Highly Toxic (USA) Very Toxic (EU). Dangerous for the
environment.
Risk Statements: Very toxic by inhalation, in contact with skin
and if swallowed. Danger of cumulative effects. Irritating to
eyes, respiratory system and skin. Very toxic to aquatic
organisms, may cause long-term adverse effects in the aquatic
environment.
Safety Statements: Keep away from food, drink, and animal
feedingstuffs. In case of contact with eyes, rinse immediately
with plenty of water and seek medical advice. After contact with
skin, wash immediately with plenty of water. Wear suitable
protective clothing. In case of accident or if you feel unwell,
seek medical advice immediately (show the label where possible).
This material and its container must be disposed of as hazardous
waste. Avoid release to the environment. Refer to special
instructions/safety data sheets.
US Statements: Neurological hazard. Target organ(s): Kidneys.
Calif. Prop. 65 developmental hazard.

UNITED STATES REGULATORY INFORMATION

SARA LISTED: Yes

NOTES: This product is subject to SARA section 313 reporting requirements - mercury compounds.

TSCA INVENTORY ITEM: Yes

UNITED STATES - STATE REGULATORY INFORMATION

CALIFORNIA PROP - 65

California Prop - 65: This product is or contains chemical(s) known to the state of California to cause developmental toxicity.

CANADA REGULATORY INFORMATION

WHMIS Classification: This product has been classified in accordance with the hazard criteria of the CPR, and the MSDS contains all the information required by the CPR.

DSL: No

NDSL: Yes

Section 16 - Other Information

DISCLAIMER

For R&D use only. Not for drug, household or other uses.

WARRANTY

The above information is believed to be correct but does not purport to be all inclusive and shall be used only as a guide. The information in this document is based on the present state of our knowledge and is applicable to the product with regard to appropriate safety precautions. It does not represent any guarantee of the properties of the product. Sigma-Aldrich Inc., shall not be held liable for any damage resulting from handling or from contact with the above product. See reverse side of invoice or packing slip for additional terms and conditions of sale. Copyright 2009 Sigma-Aldrich Co. License granted to make unlimited paper copies for internal use only.

Name: _____ Block: _____

Conversions

Complete the following conversions (significant figures used properly). Convert answers to scientific notation as well (use space after initial answer). Example provided – show work!

$1.45 \text{ km} = 1450 \text{ m} = 1.45 \times 10^3 \text{ m}$

92.00 mm = _____ km

0.06 m = _____ cm

4.11×10^{-4} km = _____ in

36.4 ft = _____ mi

0.416 mi = _____ cm

94.52 nm = _____ in

88.0 mg = _____ g

0.620 kg = _____ g

1.79×10^6 mg = _____ kg

43.5 kg = _____ lb

128.0 oz = _____ g

750 g = _____ lb

32.8 L = _____ mL

4.8 cm^3 = _____ L

7.35 gal = _____ L

82.40 mL = _____ pint

100 qt = _____ kL

2.29 cm^3 = _____ in^3

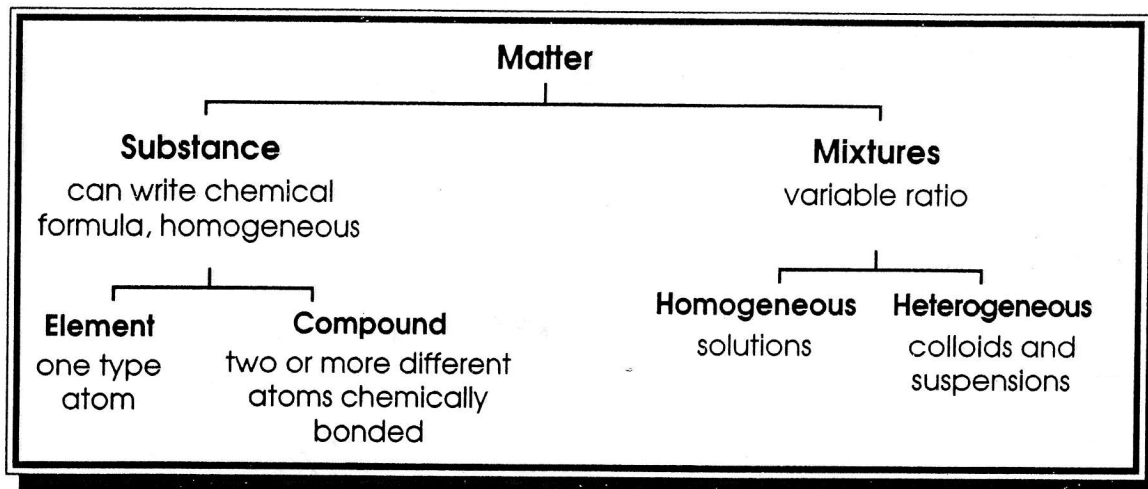
1.25 m^3 = _____ ft^3

0.0236 oz/hr = _____ mg/min

MATTER—SUBSTANCES VS. MIXTURES

Name _____

All matter can be classified as either a substance (element or compound) or a mixture (heterogeneous or homogeneous).



Classify each of the following as to whether it is a substance or a mixture. If it is a substance, write Element or Compound in the substance column. If it is a mixture, write Heterogeneous or Homogeneous in the mixture column.

Type of Matter	Substance	Mixture
1. chlorine		
2. water		
3. soil		
4. sugar water		
5. oxygen		
6. carbon dioxide		
7. rocky road ice cream		
8. alcohol		
9. pure air		
10. iron		

PHYSICAL VS. CHEMICAL PROPERTIES

Name _____

A physical property is observed with the senses and can be determined without destroying the object. For example, color, shape, mass, length and odor are all examples of physical properties.

A chemical property indicates how a substance reacts with something else. The original substance is fundamentally changed in observing a chemical property. For example, the ability of iron to rust is a chemical property. The iron has reacted with oxygen, and the original iron metal is changed. It now exists as iron oxide, a different substance.

Classify the following properties as either chemical or physical by putting a check in the appropriate column.

	Physical Property	Chemical Property
1. blue color		
2. density		
3. flammability		
4. solubility		
5. reacts with acid to form H_2		
6. supports combustion		
7. sour taste		
8. melting point		
9. reacts with water to form a gas		
10. reacts with a base to form water		
11. hardness		
12. boiling point		
13. can neutralize a base		
14. luster		
15. odor		

PHYSICAL VS. CHEMICAL CHANGES

Name _____

In a physical change, the original substance still exists, it has only changed in form. In a chemical change, a new substance is produced. Energy changes always accompany chemical changes.

Classify the following as being a physical or chemical change.

1. Sodium hydroxide dissolves in water. _____
2. Hydrochloric acid reacts with potassium hydroxide to produce a salt, water and heat. _____
3. A pellet of sodium is sliced in two. _____
4. Water is heated and changed to steam. _____
5. Potassium chlorate decomposes to potassium chloride and oxygen gas.

6. Iron rusts. _____
7. When placed in H_2O , a sodium pellet catches on fire as hydrogen gas is liberated and sodium hydroxide forms. _____
8. Evaporation _____
9. Ice melting _____
10. Milk sours. _____
11. Sugar dissolves in water. _____
12. Wood rotting _____
13. Pancakes cooking on a griddle _____
14. Grass growing in a lawn _____
15. A tire is inflated with air. _____
16. Food is digested in the stomach. _____
17. Water is absorbed by a paper towel. _____